Cell Reports, Volume *23*

Supplemental Information

A *De Novo* Mouse Model of C11orf95-RELA Fusion-Driven Ependymoma Identifies Driver Functions in Addition to NF-κB

Tatsuya Ozawa, Sonali Arora, Frank Szulzewsky, Gordana Juric-Sekhar, Yoshiteru Miyajima, Hamid Bolouri, Yoshie Yasui, Jason Barber, Robert Kupp, James Dalton, Terreia S. Jones, Mitsutoshi Nakada, Toshihiro Kumabe, David W. Ellison, Richard J. Gilbertson, and Eric C. Holland

SUPPLEMENTAL FIGURES

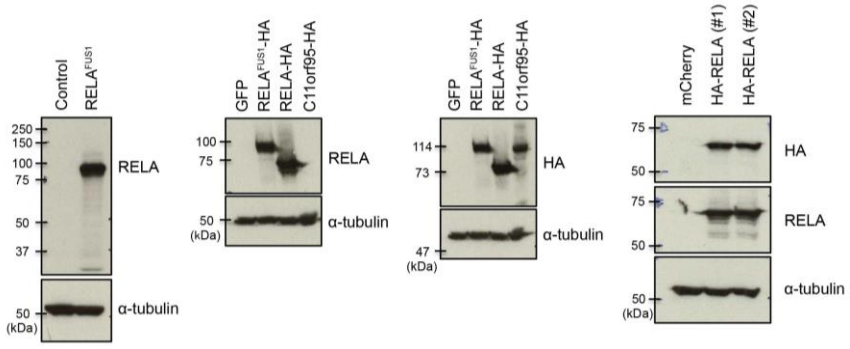

Figure S1 related to Figure 1. RCAS-C11orf95-RELA type 1 (RELA^{FUS1}), C11orf95-RELA type I-HA (RELA^{FUS1}-HA), RELA-HA, RCAS-HA-RELA and C11orf95-HA vector expression in DF-1 cells. Cell lysates of DF-1 cells infecting the relevant RCAS viruses were subjected to immunoblot analysis with the indicated antibodies.

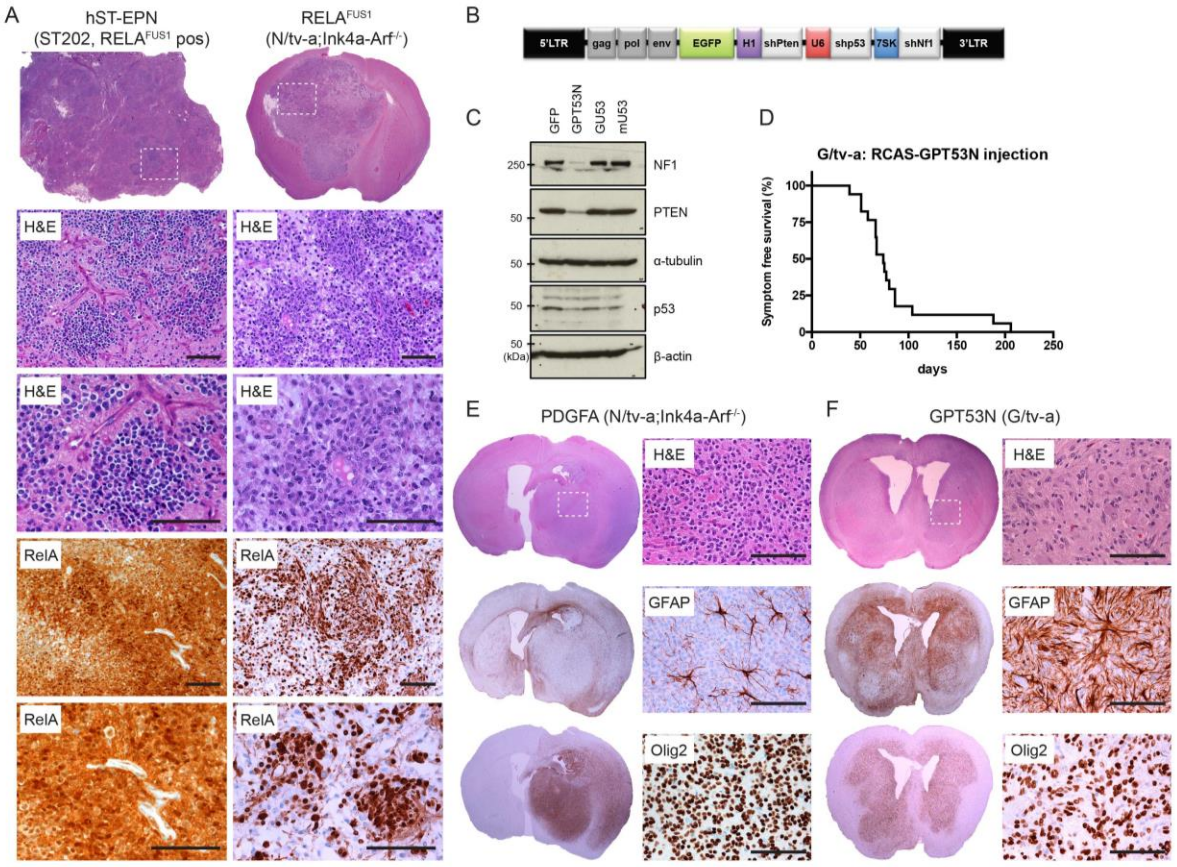

Figure S2 related to Figure 2. (A) A biphasic architectural pattern in human ST-ependymoma and mouse *RELA^{FUS1}*-induced brain tumor. Representative H&E and IHC analysis for RELA of human *RELA^{FUS1}* positive ST-ependymoma and the *RELA^{FUS1}*-induced brain tumor in *N/tv-a;Ink4a-Arf$^{-/-}$* mice are shown in the figure. Dashed boxes in upper panels denote the enlarged regions as shown in lower panels. Scale bars, 100 μm. (B) Schematic of the RCAS-GFP-shPTEN-shp53-shNF1 (GPT53N) multicistronic vector construct (C) RCAS-GPT53N vector-mediated PTEN, p53 and NF1 knockdown in 3T3T cells. Cell lysates of 3T3T cells retrovirally infecting the RCAS-GPT53N, GFP-U6-shp53 (GU53) or mCherry-U6-shp53 (mU53) virus were subjected to immunoblot blot analysis with the indicated antibodies. (D) Kaplan-Meier survival curve showing symptom-free survival of GPT53N-induced brain tumors in *G/tv-a* mice. (E and F) Representative H&E and IHC analysis with the indicated antibodies of the RCAS-PDGFA (E)- and GPT53N (F)-induced brain tumors in the indicated *tv-a* mice. All enlarged images present area of dashed boxes in H&E staining. PDGFA and GPT53N tumors also serve as positive control for Olig2 and GFAP immunohistochemistry, respectively. Scale bars, 100 μm

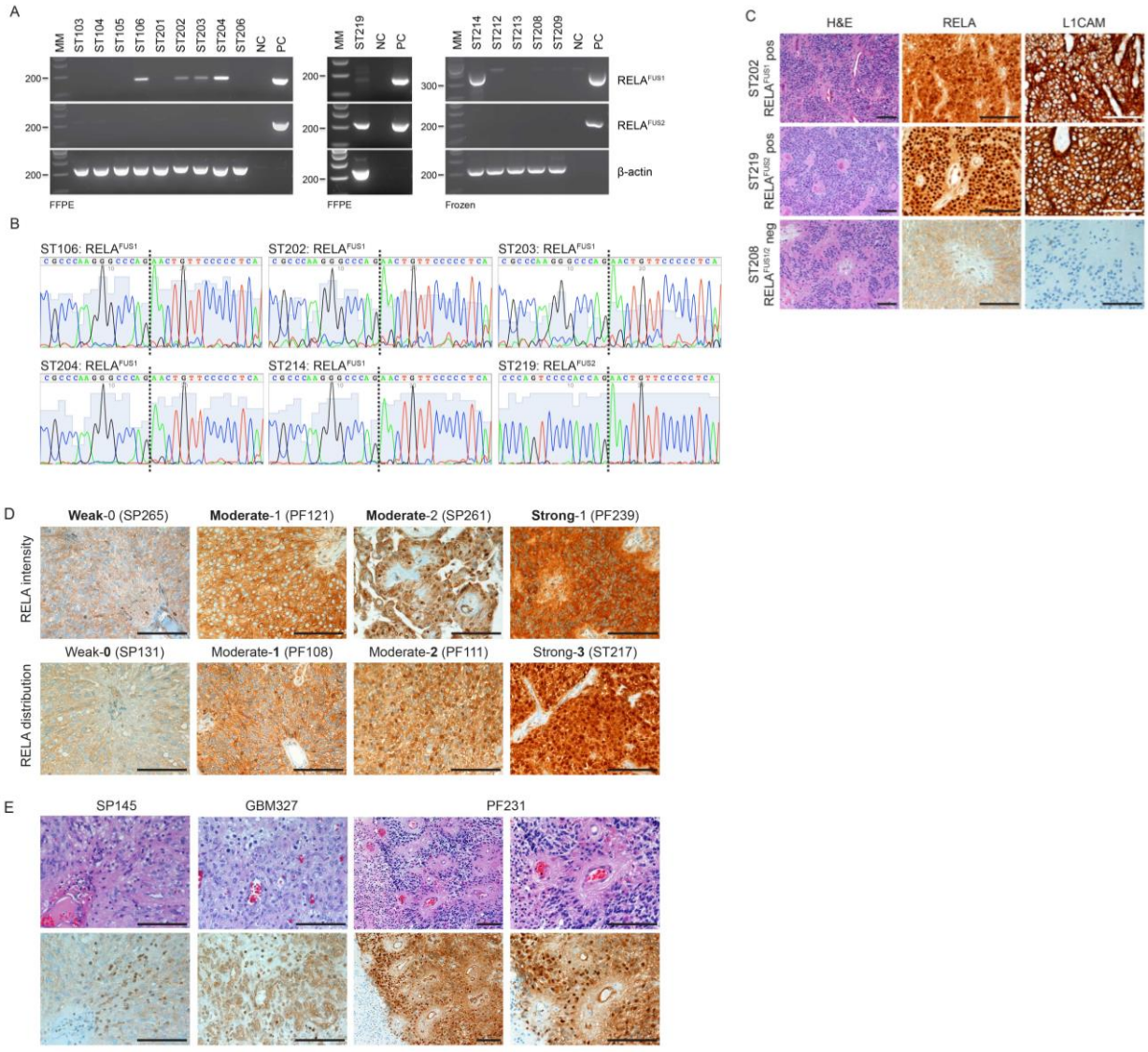

Figure S3 related to Figure 3. (A) RT-PCR detection of the RELA^{FUS1} and RELA^{FUS2} transcripts in ST-ependymomas. (B) Electropherograms of PCR products detected in ST-ependymomas. (C) Representative H&E and IHC analysis for RELA and L1CAM of human RELA^{FUS1} (ST202), RELA^{FUS2} (ST219) positive and negative (ST208) ST-ependymomas. All IHC images were shown the same area as each H&E images. Scale bars, 100 μm. (D) Semi-quantitative IHC analysis in human ependymomas. Representative images corresponding to the criteria for RELA IHC analysis were shown in the figure. Scale bars, 100 μm (E) Representative images of RELA-IHC in immune cells (SP145), endothelial cells (GBM327) and around necrotic areas (PF231). Scale bars, 100 μm

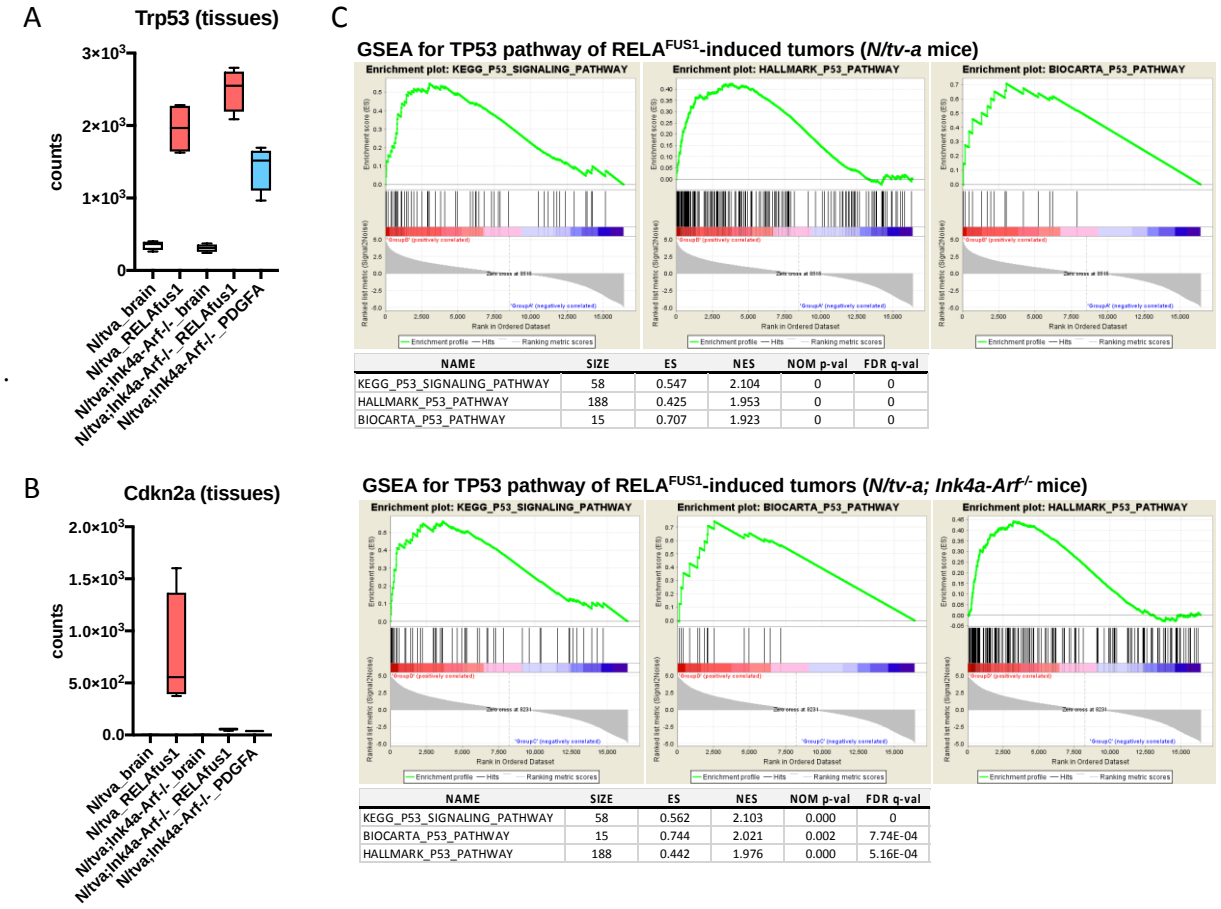

NAME	SIZE	ES	NES	NOM p-val	FDR q-val
KEGG_P53_SIGNALING_PATHWAY	58	0.547	2.104	0	0
HALLMARK_P53_PATHWAY	188	0.425	1.953	0	0
BIOCARTA_P53_PATHWAY	15	0.707	1.923	0	0

NAME	SIZE	ES	NES	NOM p-val	FDR q-val
KEGG_P53_SIGNALING_PATHWAY	58	0.562	2.103	0.000	0
BIOCARTA_P53_PATHWAY	15	0.744	2.021	0.002	7.74E-04
HALLMARK_P53_PATHWAY	188	0.442	1.976	0.000	5.16E-04

Figure S4 related to Figure 4. (A) and (B) Box plots of *Trp53* and *Cdkn2a* gene expression in mouse control brains and brain tumor tissues. (C) Gene set enrichment analysis (GSEA) for TP53 pathway of *RELA*^{FUS1}-induced tumor (in comparison to the respective control brains) in *N/tv-a* and *N/tv-a; Ink4a-arf*$^{-/-}$ mice. Gene expression profiles of these samples were compared using the three TP53-related gene sets as indicated in the figure (Mootha et al., 2003; Subramanian et al., 2005). The nominal p value (NOM p-val) and false discovery rate (FDR)-corrected q value (FDR q-val) are indicated in the Tables. A nominal p-value of <0.05 was considered significant in this analysis. SIZE denotes number of genes in the gene set after filtering out those genes not in the expression dataset. ES, Enrichment score; NES, Normalized enrichment score.

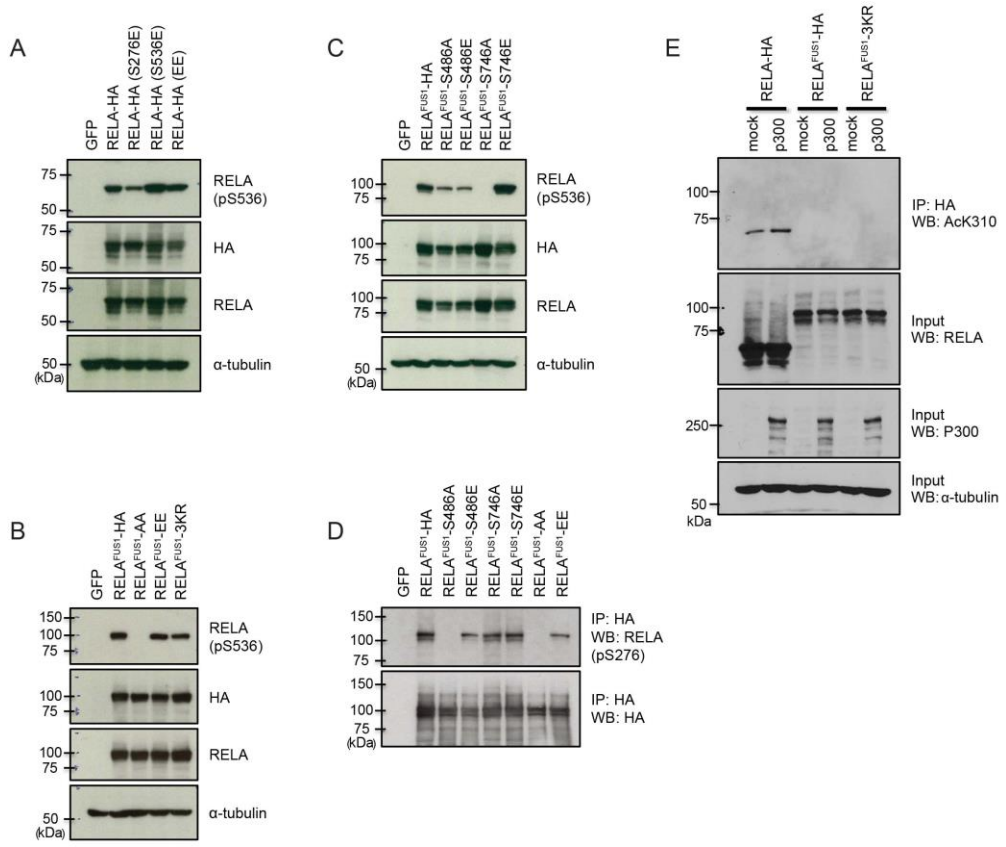

Figure S5 related to Figure 5. (A) Phosphorylation status at Ser536 of RELA-HA and the mutants. DF-1 cells infecting the relevant RCAS viruses were maintained at regular culture condition and the cell lysates were then subjected to immunoblot analysis with the indicated antibodies. RELA-HA (EE) denotes RELA-HA-S276/536E mutant. (B and C) Phosphorylation status at Ser746 (corresponding to RELA-Ser536) of RELA^{FUS1}-HA and the mutants. DF-1 cells infecting the relevant RCAS viruses were maintained at regular culture condition and the cell lysates were then subjected to immunoblot analysis with the indicated antibodies as well. RELA^{FUS1}-AA, -EE and -3KR denote RELA^{FUS1}-HA-S486/746A, S486/746E and K428R/K431R/K520R mutants, respectively. (D) Phosphorylation status at Ser486 (corresponding to RELA-Ser276) of RELA^{FUS1}-HA and the mutants. For phospho-Ser486 detection, cell lysates were immunoprecipitated with anti-HA agarose and were then subjected to immunoblot analysis with phospho-Ser276 RELA antibody, followed by re-probed with anti-HA-tag antibody. (E) Acetylation status at K310 in RELA-HA or at K520 (corresponding to RelA-K310) in the RELA^{FUS1}-HA and RELA^{FUS1}-3KR (K428R/K431R/K520R) mutants. Cell lysates of DF-1 cells transiently transfected with pcDNA3.1 empty vector or pCMVβ-p300-myc vector were immunoprecipitated with anti-HA-Agarose antibody and then subjected to immunoblot analysis with the indicated antibodies.

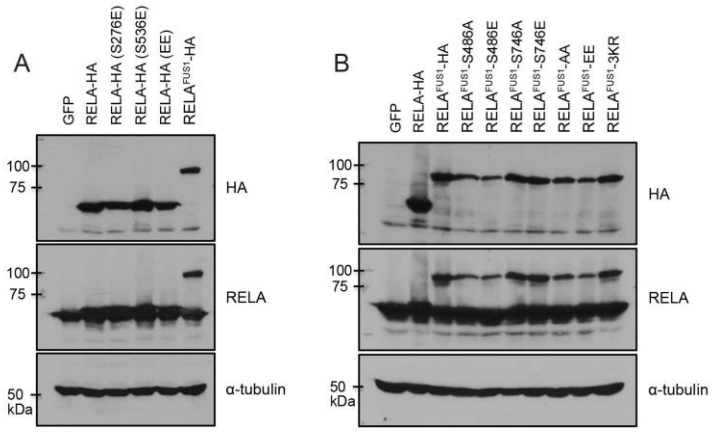

Figure S6 related to Figure 6. (A and B) Immunoblot analysis of 3T3T cells expressing GFP, RELA-HA, RELA mutants, RELA^{FUS1}-HA or RELA^{FUS1}-HA mutants. Cells were retrovirally infected with various RCAS viruses as described and the cell lysates were then subjected to immunoblot analysis with the indicated antibodies.

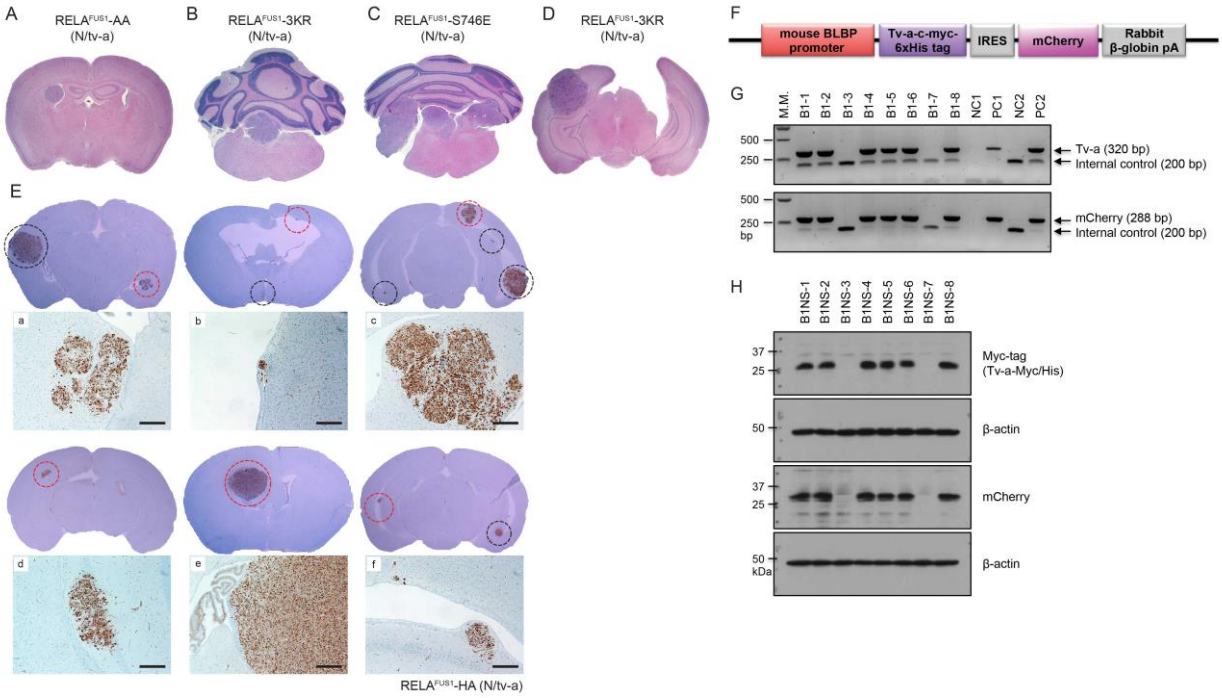

Figure S7 related to Figure 7. (A-D) Representative H&E images of the RCAS-RELA^{FUS1}-S486/746A (A), RELA^{FUS1}-3KR (B and D) and RELA^{FUS1}-S746E (C)-induced brain tumors in *N/tv-a* mice. (E) Immunohistochemical analysis for HA tag of the RCAS-RELA^{FUS1}-HA-induced brain tumors in *N/tv-a* mice (Also see Fig. 7A). Neonatal pups were sacrificed at 1 month post-injection and the brain sections were then subjected to IHC for HA tag staining. Dashed circles in upper panels show early lesions or brain tumors representing essentially the RCAS vector expression. Red dashed circles denote the enlarged regions as shown in lower panels. Scale bars, 100 μm. (F) Schematic of the *BLBP (B)/tv-a* transgene construct (G) PCR genotyping of *B/tv-a* mice. DNAs were extracted from tails of eight newborn pups (B1-1 ~ 8) and then subjected to PCR analysis using primer pairs specific for tv-a or mCherry with internal positive control. Water (lane 9: NC1), the original B/tv-a transgene plasmid (lane 10: PC1), tail DNA of both tv-a and mCherry negative (lane 11: NC2) and positive mouse (lane 12: PC2) were used for control samples in the PCR analysis. (H) Tv-a and mCherry protein expression in neurospheres derived from *B/tv-a* mice (B1 line). Neurospheres (B1NS1 ~ 8) were generated by mechanical dissociation with forebrains of eight newborn pups genotyped in Figure S7G and the protein extracts were subjected to immunoblot analysis with the indicated antibodies.

SUPPLEMENTAL EXPERIMENTAL PROCEDURES

Cell culture and transfections

DF-1 cells (ATCC: CRL-12203) were maintained according to the manufacture's protocol. RCAS viruses were produced in DF-1 packaging cells and were maintained with minor modification for brain tumor formation as described previously (Holland et al., 2000; Holland et al., 1998; Holland and Varmus, 1998; Ozawa et al., 2014). *B/tv-a* neurospheres were generated by mechanical dissociation from forebrains of neonatal pups in *B/tv-a* mice and then maintained as a floating culture in serum free neurosphere medium (Stem Cell Technologies) (Charles et al., 2010). NIH-3T3/tv-a (3T3T) cells were previously described (Ozawa et al., 2014). Test for Mycoplasma contamination has not been performed for these cell lines.

H&E staining and Immunohistochemistry (IHC)

The following primary antibodies were used for the IHC: HA (Roche, 11867423001), GFAP (DAKO, Z0334), Olig2 (MILLIPORE, AB9610), GFP (Invitrogen, A11122), PTEN (#9188, Cell Signaling Technology), RELA (#8242, Cell Signaling Technology) and PDGFA (sc-128, Santa Cruz Biotechnology, Inc.). IHC for L1CAM was performed at St. Jude Children research hospital as previously described (Parker et al., 2014). The histological diagnosis and tumor grade of murine tumors were established based on the World Health Organization (WHO) criteria (Huse et al., 2009; Louis et al., 2007; Louis et al., 2016). The murine brains were evaluated the protein expression pattern and level between multiple murine brain tumors or no RCAS virus-injected control brains (at least 4 tumors or normal brains for each tumor types).

Human brain tumors from three institutional archives (Tabls S2A) were diagnosed as ependymoma or GBM by pathological review at each university. All ST-ependymomas were secondarily reviewed by D.W.E., and several discrepancies in the histological diagnosis were identified between initial diagnosis and review (Table S2C). For RELA immunohistochemical analysis of human brain tumor samples, we evaluated cytoplasmic or nuclear immunoreactivity, as well as staining intensity (Table S2B). In the analysis for staining intensity, the protein expression level was evaluated irrespective of the subcellular localization. Labeling of the tumor samples was evaluated by the investigators: G.J.S. and T.O. in a semi-quantitative manner. After evaluation, cases with dubious scoring were discussed by two investigators (T.O. and G.J.S.) together to reach a consensus. Of note, dominant cytoplasmic staining of RELA occasionally accompanying nuclear immunopositivity, and intra- and/or perinuclear staining of RELA were commonly detected in immune cells and endothelial cells, respectively (Fig. S3E). Further obvious nuclear immopositivity was sometimes identified in immune cells and/or tumor cells adjacent to necrotic areas (Fig. S3E). Gemistocytes in GBMs commonly presented remarkable strong cytoplasmic RELA immunopositivity (data not shown). Thus, although all tumors, including both ependymomas and GBMs, showed extensive cytoplasmic staining accompanying nuclear immunopositivity with various degrees, an intense nuclear staining for RELA classified as the criteria: Strong-3 was detected in only 9 ST-EPNs in our study (Fig. 3B, C, S3D and Table S2C). Then, to determine whether the characteristic nuclear pattern of RELA immunostaining was

associated with the *RELA*^{FUS} gene, we analyzed all ST-ependymomas with interphase fluorescence in situ hybridization (iFISH) for *RELA*^{FUS} and/or RT-PCR for *RELA*^{FUS1} and *RELA*^{FUS2} (Parker et al., 2014). Gene rearrangement of chromosome 11 consisting of the fusion and/or the fusion transcript were detected in 9 out of 23 ST-EPNs (Table S2C). Subsequent sequencing analysis of the RT-PCR products could confirm RELA^{FUS1} or RELA^{FUS2} transcript in 6 of that cases (Fig. S3A, B and Table S2C). These fusion-positive tumors were histologicaly associated with a vascular or clear cell phenotype, consistent with previous studies (Figarella-Branger et al., 2016; Parker et al., 2014). Both iFISH and PCR detection failed in the ST216 and ST217 (recurrent case of ST216) which presented intense RELA nuclear immunoreactivity categorized as the Strong-3, probably due to very old FFPE samples (over 30 years ago samples) (Table S2C). However immunoreactivity for L1CAM was successfully detected in the ST217 case (data not shown). Given that L1CAM immunopositivity is good correlation of RELA^{FUS} in ST-ependymoma (Fig. S3C) (Parker et al., 2014), both ST216 and ST217 was highly suggested to be positive for the *RELA*^{FUS}. Unexpectedly, L1CAM immunostaining and iFISH for the *RELA*^{FUS} were positive in ST212 in spite of no obvious nuclear immunopositivity for RELA and no RELA^{FUS1} and RELA^{FUS2} transcript in RT-PCR analysis. However the ST211 (primary case of ST212) and ST213 (recurrent case of ST212) was negative for RT-PCR or iFISH analysis. Further, the ST211 case presented an infiltrative high-grade glioma morphology, containing extensive pseudopapillary formations, which was not typical of the ST-ependymoma phenotypes, strongly suggesting that this case might not be driven by the *RELA*^{FUS} though the gene rearrangement occurred in parts. Further, iFISH suggested possible *RELA* gene rearrangement without *C11orf95* in ST218 case. However the case is also not likely to be driven by the *RELA*^{FUS} as supported by no characteristic nuclear immunoreactivity of RELA, atypical histological phenotype to the fusion positive case (Fig. 3B and Table S2C) and negative for RELA^{FUS1} and RELA^{FUS2} transcripts as well.

Plasmids

The pCEXRFP-C11orf95-RELA type I fusion (RELA^{FUS1}), RELA and C11orf95 plasmids were kindly provided by Dr. Richard Gilbertson. For generation of the RCAS- RELA^{FUS1} vector, the coding sequence (CDS) was subcloned into pENTR1A Dual Selection vector (life technologies) as between the BamHI and NotI sites and then transferred into RCAS destination vector (Loftus et al., 2001) using the LR recombination according to the manufacture's protocol (life technologies). RELA CDS was PCR-amplified to add the HA epitope tag in the N- or C-terminus portion and then subcloned into pENTR/D-TOPO vector (life technologies), followed by transferred into the RCAS destination vector as well. HA epitope tag of the pENTR1A-RELA^{FUS1}-HA and pENTR1A-C11orf95-HA vector was added by replacing the C-terminal portion of the RELA-HA sequence as between EcoRI and PmeI/EcoRV sites or by linker ligation as between BssSI and NotI sites, respectively, followed by transferred into the RCAS destination vector.

RELA-HA mutants were generated with PCR-amplification to add HA tag and/or site-directed mutagenesis (QuikChange II XL Site-Directed Mutagenesis Kit, Agilent Technologies) to add point mutation(s) using

original RELA mutant constructs as listed (Table S1E). These RELA mutants were subcloned in entry vector, were then transferred into the RCAS destination vector as well. RCAS-RELA^{FUS1}-HA mutants were generated by replacing the C-terminal RELA fragment of RELA^{FUS1} with the relevant RELA-HA mutant. T7-RelA (S276E, Addgene plasmid # 24154), T7-RelA (S536E, Addgene plasmid # 24156), T7-RelA (S276A, Addgene plasmid # 24153) and T7-RelA (KR, Addgene plasmid # 23251) were a gift from Dr. Warner Greene.

For generation of RCAS-GPT53N (GFP-shPTEN-shp53-shNF1) multicistronic vector (Fig. S2B), GFP (pMXs-IRES-GFP Retroviral Vector, CELL BIOLABS, INC.), shPTEN driven by H1 promoter (pSUPER.retro.puro, OligoEngine), shp53 driven by U6 promoter (pLKO.1, MSKCC HTP facility) and shNF1 driven by 7SK promoter (psiRNA-h7SKGFPzeo, InvivoGen) were assembled in pENTR1A Dual Selection vector (Invitrogen) and were then transferred using the LR recombination into the RCAS destination vector. Target sequence for shPTEN (#2), shp53 (696) and shNF1 (249) were previously described (Ozawa et al., 2014). For RCAS-GFP-U6-shp53 (GU53) and mCherry-U6-shp53 (mU53), GFP, mCherry, shp53 driven by U6 promoter were assembled using the LR recombination in the RCAS destination vector as well. TurboGFP was PCR-amplified from pGIPZ vector (Genomics Shared Resource in the FHCRC) and then subcloned in RCAS-Y vector. pcDNA3.1/myc-His B was obtained from Invitrogen (V800-20). pCMVβ-p300-myc was a gift from Dr. Tso-Pang Yao (Addgene plasmid # 30489).

***BLBP (B)/tv-a* transgenic mouse**

The *B/tv-a* transgene is a 4kb fragment of mouse BLBP promoter (1.6 kb 5' flanking sequence) driving expression of the quail tv-a cDNA tagged with c-myc-6xHis in the C-terminus, the IRES-mCherry cDNA and a fragment from rabbit *β-globin* gene supplying an intron and signal for polyadenylylation (Fig. S7F) (Feng and Heintz, 1995). The construct was assembled by replacing the transgene fragments in the pCAG-CAT-LSL-pA vector (Araki et al., 1995). Loss (G or T in 17Gs or 9Ts repeat, respectively) or addition (G in the 13Gs repeat) of each one nucleotide in three parts of 17 guanines, 9 thymines and 13 guanines repeat sequence of the *BLBP* promoter was found. Production of the *B/tv-a* mouse line was by pronuclear injection (B6C3 embryo donors) of the *B/tv-a* transgene, which had been released from the plasmid by digestion with SalI and SmaI, at the Transgenic Resources Program in University of Washington. Pronuclear injection generated five chimera founders with germ-line transmission (B1-5 lines). All were phenotypically normal, viable and fertile but the transgene from B4 line was not transferred to next generation. Therefore, four founders were then repeatedly back-crossed to C57BL/6J mice (The Jackson laboratory). After initial functional characterization for *Tv-a*, one *B/tv-a* mouse line (B1 line) was chosen for further analysis and these mice after third generations were presented for the RCAS-mediated brain tumor formation in this study.

Genotyping was carried out on DNA purified from tail biopsies after PCR reactions was performed with *Taq* DNA polymerase (Invitrogen #18038-042) and primer pairs specific for Tv-a, Tva5 (5-CTGCTGCCCGGTAACGTGACCGG-3) and Tva-AS3 (5-CTCACCAGCTCACAGCAAAA-3), or for mCherry, MC9703 (5-AGGACGGCGAGTTCATCTAC-3) and MC9704 (5-TGGTGTAGTCCTCGTTGTGG-3) (The Jackson laboratory) with internal positive control primer pair, oIMR8744 (5-CAAATGTTGCTTGTCTGGTG-3) and oIMR8745 (5-GTCAGTCGAGTGCACAGTTT-3) (The Jackson laboratory). The PCR amplification was performed in a 10-μl reaction volume under the following conditions: 1 x PCR Buffer minus Mg, dNTP mix (0.2 mM each), 1.5 mM $MgCl_2$, two primer pairs (0.5 μM each), *Taq* DNA Polymerase (2.5 unit), 5% DMSO, 1 μl of DNA (approximately 50ng) and autoclaved distilled water up to 10 μl. The protocol was 5 min at 94°C, denaturation for 45 sec at 94°C, annealing for 30 sec at 57°C, and extension for 60 sec at 72°C for 35 cycles, followed by 10 min of final extension. Subsequently, the PCR products were resolved by electrophoresis on 1.5% agarose gel with SYBR Safe DNA Gel Stain (Invitrogen) (Fig. S7G).

Electron microscopic analysis and Interphase fluorescence in situ hybridization (iFISH)

These analyses were performed as previously described (Parker et al., 2014).

Detection of RELA^{FUS1} and RELA^{FUS2} transcripts

The identification of the RELA^{FUS1} and RELA^{FUS2} in human ST-ependymomas was performed using RT-PCR analysis with minor modifications according to the protocol as previously reported (Cachia et al., 2015; Parker et al., 2014). Total RNAs from frozen or FFPE samples were isolated with the RNeasy Minikit (Qiagen, CA, USA) or the Master Pure Complete DNA or RNA Purification Kit (Illumina Inc., San Diego, CA, USA), respectively and were then used to synthesize cDNAs by using the SuperScript VILO Master Mix (life technologies, CA, USA) according to the manufacturer's protocol. The RNA quality was evaluated with β-actin amplification in subsequent RT-PCR analysis. When detected β-actin but not RELA^{FUS1} and/or RELA^{FUS2} transcript, the case was defined as negative for the fusion in this study. The primers for the RELA^{FUS1} and RELA^{FUS2} detection are previously described (Parker et al., 2014). Primer pair, HACT-F1: 5-GGACTTCGAGCAAGAGATGG-3 and HACT-R1: 5-AGCACTGTGTTGGCGTACAG-3 was used for human β-actin amplification, serving as an internal control. The RT-PCR amplification was performed with GoTaq Long PCR Master Mix (Promega). The PCR cycles were as follows: initial denaturation at 95 °C for 2 min followed by 35 cycles of 30 s at 92 °C and 60 s at 63 °C and a final extension was performed for 10 min at 72 °C. The PCR products were purified using the Qiaquick PCR purification Kit (Qiagen) and/or QIAquick Gel Extraction Kit (Qiagen), and then submitted to direct sequencing on an ABI 3730xl DNA analyzer (Applied Biosystems, Foster City, CA, USA) (Fig. S3A and B).

Western blot analysis

For preparation of the cellular lysates, cells were solubilized with lysis buffer as follows: 20 mM Tris-HCl, pH 7.5, 5 mM $MgCl_2$, 150 mM NaCl, 1 mM EDTA, 1% Nonidet P-40, 2mM NaF, 1mM $NaVO_3$ and protease inhibitor cocktail (Sigma-Aldrich). Western blots were developed using ECL Detection Reagents (GE Healthcare). The following primary antibodies were used for Western blots: Neurofibromin (sc-67, Santa Cruz Biotechnology); Phospho-NF-κB p65 (Ser276) (sc-101749, Santa Cruz Biotechnology); p53 (NCL-p53-CM5P, Novacastra); α-tubulin (T 9026, Sigma-Aldrich); β-actin (A1978, Sigma-Aldrich); c-Myc (M4439, Sigma-Aldrich); PTEN (Cell Signaling Technology, #9188); p65/RelA (Cell Signaling Technology, #8242); Phospho-NF-κB p65 (Ser536) (Cell Signaling Technology, #3033); Acetyl-NF-kB p65 (Lys310) (Cell Signaling Technology, #3045); mCherry (ThermoFisher Scientific, M11217); p300 (Bethyl, A300-358A) and HA (Roche, 11867423001). All western blot analyses were performed at least twice and successfully repeated in the experiments. The representative images were shown in the figures. Figure S7H was performed once. C11orf95-HA and tv-a-myc/His expression were evaluated with HA- and myc-tag antibodies because of no available antibody against C11orf95 and tv-a, respectively.

Immunoprecipitation analysis for phospho-Ser486 detection of $RELA^{FUS1}$ corresponding to Ser276 of RELA

DF1 cells expressing the relevant RCAS viruses were processed as described in **Western blot analysis** and the lysates were then immunoprecipitated with monoclonal anti-HA-Agarose antibody (A2095, Sigma-Aldrich) for three hours. Subsequent immunoblots were probed with the indicated antibodies.

Immunoprecipitation analysis for acethylated-Lys520 (AcK520) detection of $RELA^{FUS1}$ corresponding to Lys310 of RELA

DF-1 cells expressing the relevant RCAS viruses were transiently transfected with pcDNA3.1 empty vector or pCMVβ-p300-myc vector. After 48 hours of the transfection, cells were harvested and processed as described in **Western blot analysis** and the cell lysates were then immunoprecipitated with monoclonal anti-HA-Agarose antibody (A2095, Sigma-Aldrich) for two hours. Subsequent immunoblots were probed with the indicated antibodies.

Principal Component Analysis (PCA)

For the sample similarity plot of Fig. 4A, The R function prcomp was used to calculate Principal Components, which was visualized using R package ggplot2 (Wickham, 2009).

Gene Set Enrichment Analysis (GSEA)

GSEA was performed using the GenePattern GSEA module from the Broad Institute (http://genepattern.broadinstitute.org/). For GSEA comparison of our mouse tumors to the human SJEPDs, we converted all mouse gene symbols to human using the MGI homology map

(http://www.informatics.jax.org/homology.shtml). We also converted mouse RNA-seq read count data to RPKM (Bioconductor package 'edgeR') for compatibility with the human data. Gene sets for human ependymomas are previously described (Table S3C) (Taylor et al., 2005).

Multidimensional scaling (MDS)

For the sample similarity plot of Fig. 6A, we first used the R function dist to calculate Euclidean distance between samples, then used the R command 'cmdscale' for Classical Multi-Dimensional Scaling which was visualized using R package ggplot2 (Wickham, 2009).

Hypergeometric Test

Hypergeometric tests were conducted in R using R function phyper to test if the overlap between the two gene lists was significant.

SUPPLEMENTAL REFERENCES

Araki, K., Araki, M., Miyazaki, J., and Vassalli, P. (1995). Site-specific recombination of a transgene in fertilized eggs by transient expression of Cre recombinase. Proceedings of the National Academy of Sciences of the United States of America *92*, 160-164.

Cachia, D., Wani, K., Penas-Prado, M., Olar, A., McCutcheon, I. E., Benjamin, R. S., Armstrong, T. S., Gilbert, M. R., and Aldape, K. D. (2015). C11orf95-RELA fusion present in a primary supratentorial ependymoma and recurrent sarcoma. Brain tumor pathology *32*, 105-111.

Charles, N., Ozawa, T., Squatrito, M., Bleau, A. M., Brennan, C. W., Hambardzumyan, D., and Holland, E. C. (2010). Perivascular nitric oxide activates notch signaling and promotes stem-like character in PDGF-induced glioma cells. Cell stem cell *6*, 141-152.

Feng, L., and Heintz, N. (1995). Differentiating neurons activate transcription of the brain lipid-binding protein gene in radial glia through a novel regulatory element. Development *121*, 1719-1730.

Figarella-Branger, D., Lechapt-Zalcman, E., Tabouret, E., Junger, S., de Paula, A. M., Bouvier, C., Colin, C., Jouvet, A., Forest, F., Andreiuolo, F., *et al.* (2016). Supratentorial clear cell ependymomas with branching capillaries demonstrate characteristic clinicopathological features and pathological activation of nuclear factor-kappaB signaling. Neuro-oncology.

Holland, E. C., Celestino, J., Dai, C., Schaefer, L., Sawaya, R. E., and Fuller, G. N. (2000). Combined activation of Ras and Akt in neural progenitors induces glioblastoma formation in mice. Nat Genet *25*, 55-57.

Holland, E. C., Hively, W. P., DePinho, R. A., and Varmus, H. E. (1998). A constitutively active epidermal growth factor receptor cooperates with disruption of G1 cell-cycle arrest pathways to induce glioma-like lesions in mice. Genes Dev *12*, 3675-3685.

Holland, E. C., and Varmus, H. E. (1998). Basic fibroblast growth factor induces cell migration and proliferation after glia-specific gene transfer in mice. Proc Natl Acad Sci U S A *95*, 1218-1223.

Huse, J. T., Brennan, C., Hambardzumyan, D., Wee, B., Pena, J., Rouhanifard, S. H., Sohn-Lee, C., le Sage, C., Agami, R., Tuschl, T., and Holland, E. C. (2009). The PTEN-regulating microRNA miR-26a is amplified in high-grade glioma and facilitates gliomagenesis in vivo. Genes Dev *23*, 1327-1337.

Loftus, S. K., Larson, D. M., Watkins-Chow, D., Church, D. M., and Pavan, W. J. (2001). Generation of RCAS vectors useful for functional genomic analyses. DNA research : an international journal for rapid publication of reports on genes and genomes *8*, 221-226.

Louis, D. N., Ohgaki, H., Wiestler, O. D., Cavenee, W. K., Burger, P. C., Jouvet, A., Scheithauer, B. W., and Kleihues, P. (2007). The 2007 WHO classification of tumours of the central nervous system. Acta neuropathologica *114*, 97-109.

Louis, D. N., Perry, A., Reifenberger, G., von Deimling, A., Figarella-Branger, D., Cavenee, W. K., Ohgaki, H., Wiestler, O. D., Kleihues, P., and Ellison, D. W. (2016). The 2016 World Health Organization Classification of Tumors of the Central Nervous System: a summary. Acta neuropathologica *131*, 803-820.

Mootha, V. K., Lindgren, C. M., Eriksson, K. F., Subramanian, A., Sihag, S., Lehar, J., Puigserver, P., Carlsson, E., Ridderstrale, M., Laurila, E., *et al.* (2003). PGC-1alpha-responsive genes involved in oxidative phosphorylation are coordinately downregulated in human diabetes. Nat Genet *34*, 267-273.

Ozawa, T., Riester, M., Cheng, Y. K., Huse, J. T., Squatrito, M., Helmy, K., Charles, N., Michor, F., and Holland, E. C. (2014). Most Human Non-GCIMP Glioblastoma Subtypes Evolve from a Common Proneural-like Precursor Glioma. Cancer cell *26*, 288-300.

Pajtler, K. W., Witt, H., Sill, M., Jones, D. T., Hovestadt, V., Kratochwil, F., Wani, K., Tatevossian, R., Punchihewa, C., Johann, P., *et al.* (2015). Molecular Classification of Ependymal Tumors across All CNS Compartments, Histopathological Grades, and Age Groups. Cancer cell *27*, 728-743.

Parker, M., Mohankumar, K. M., Punchihewa, C., Weinlich, R., Dalton, J. D., Li, Y., Lee, R., Tatevossian, R. G., Phoenix, T. N., Thiruvenkatam, R., *et al.* (2014). C11orf95-RELA fusions drive oncogenic NF-kappaB signalling in ependymoma. Nature *506*, 451-455.

Subramanian, A., Tamayo, P., Mootha, V. K., Mukherjee, S., Ebert, B. L., Gillette, M. A., Paulovich, A., Pomeroy, S. L., Golub, T. R., Lander, E. S., and Mesirov, J. P. (2005). Gene set enrichment analysis: a knowledge-based approach for interpreting genome-wide expression profiles. Proc Natl Acad Sci U S A *102*, 15545-15550.

Taylor, M. D., Poppleton, H., Fuller, C., Su, X., Liu, Y., Jensen, P., Magdaleno, S., Dalton, J., Calabrese, C., Board, J., *et al.* (2005). Radial glia cells are candidate stem cells of ependymoma. Cancer cell *8*, 323-335.

Wickham, H. (2009). ggplot2: Elegant graphics for data analysis, (New York: Springer).